GEOPHYSICS, VOL. 91, NO. 4 (JULY-AUGUST 2026); P. A43–A49, 4 FIGS.
10.1190/GEO-2025-1024

Representations for multidimensional down-down deconvolution of ocean-bottom seismic data: Theory and practical implications

Kees Wapenaar[1], Matteo Ravasi[2], and Claudio Bagaini[3]

ABSTRACT

Multidimensional up-down deconvolution effectively eliminates surface-related multiples from ocean-bottom seismic data. Recently, several down-down deconvolution methods have been introduced as attractive alternatives. Although multidimensional up-down deconvolution fully accounts for lateral variations of the medium parameters, the underlying theory of some of the down-down deconvolution methods is essentially based on the assumption that the medium is horizontally layered. Using reciprocity theory, this assumption is circumvented. This leads to representations for either receiver-side or source-side multidimensional down-down deconvolution. Compared with multidimensional up-down deconvolution, receiver-side down-down deconvolution only uses the downgoing part of the wavefield that better samples the shallow subsurface, but it is not entirely data-driven. Source-side down-down deconvolution benefits from the better-sampled source array, but in the presence of sparsely sampled receivers, it requires solving an underdetermined system of linear equations.

INTRODUCTION

Up-down deconvolution is an effective method to eliminate surface-related multiples from ocean-bottom seismic (OBS) data. An early version assumes that the medium is horizontally layered (Sonneland and Berg, 1987). Amundsen (1999) and Wapenaar et al. (2000) formulate representations for multidimensional up-down deconvolution, which hold for arbitrarily inhomogeneous media.

To tackle illumination issues of shallow reflectors, Hampson and Szumski (2020), Caprioli and Kristiansen (2021), and Lokshtanov et al. (2024) propose down-down deconvolution as an alternative to up-down deconvolution. Although they apply their methodology to OBS data from laterally varying media, their theory is essentially restricted to horizontally layered media. In this paper, we derive a new representation for multidimensional down-down deconvolution. This generalizes the theory of the aforementioned authors to the situation of arbitrarily inhomogeneous media. Because the integrals are along the receiver array, we call this a representation for receiver-side multidimensional down-down deconvolution. We compare this with representations for source-side multidimensional down-down deconvolution, as proposed by Boiero et al. (2023) and Wang and Ravasi (2024). In the discussion section, we discuss the pros and cons of each scheme.

REVIEW OF 1D DOWN-DOWN DECONVOLUTION

We start with a brief review of the down-down deconvolution approach, proposed by Hampson and Szumski (2020) and modified by Caprioli and Kristiansen (2021) and Lokshtanov et al. (2024) for the situation of OBS data. Figure 1 schematically shows the wavefields in a horizontally layered OBS configuration. Here, S is the source wavefield (including the free-surface ghost), reaching the ocean bottom from above, $R^{\cup}$ is the reflection response of

Manuscript received by the Editor 18 September 2025; revised manuscript received 23 January 2026; published ahead of production 16 June 2026; published online 1 July 2026.
[1]Delft University of Technology, Department of Geoscience and Engineering, Stevinweg 1, 2628 CN Delft, The Netherlands. E-mail: c.p.a.wapenaar@tudelft.nl (corresponding author).
[2]Shearwater GeoServices, Gatwick, United Kingdom. E-mail: matteoravasi@gmail.com.
[3]SLB, Milan, Italy. E-mail: bagaini0@slb.com.

the layered solid medium (without free-surface reflections) for sources and receivers just above the ocean bottom, and $R^\cap$ is the reflectivity of the free surface, including the propagation paths through the water layer. In the rayparameter-frequency domain, the total downgoing wavefield D just above the ocean bottom (indicated by the red ellipses in Figure 1) is given by

$$\begin{aligned} D &= S + R^\cap R^\cup S + (R^\cap R^\cup)^2 S + \cdots \\ &= (1 - R^\cap R^\cup)^{-1} S. \end{aligned} \tag{1}$$

In the rayparameter-frequency domain, all quantities in this equation are scalar functions. Hence, the products are simple scalar products, corresponding to temporal convolutions (per rayparameter) in the rayparameter-time domain.

With some simple manipulations, equation 1 can be rewritten as

$$D - S = R^\cap R^\cup D. \tag{2}$$

We are interested in retrieving the reflection response $R^\cup$ of the solid medium (i.e., without free-surface reflections). Assuming the acoustic pressure and the vertical component of the particle velocity are measured at the ocean bottom, the downgoing wavefield D just above the ocean bottom can be obtained by acoustic decomposition. Assuming the source and the parameters of the water layer are known, S and $R^\cap$ can be obtained by numerical modeling. With these quantities given, $R^\cup$ follows from $R^\cup = (D - S)/R^\cap D$. Hence, in the rayparameter-frequency domain, $R^\cup$ is retrieved by dividing the muted downgoing field $D - S$ by the scaled downgoing field $R^\cap D$. Alternatively, $R^\cap R^\cup$ follows from $R^\cap R^\cup = (D - S)/D$. Both approaches correspond to 1D down-down deconvolution per rayparameter (i.e., per plane wave) in the rayparameter-time domain.

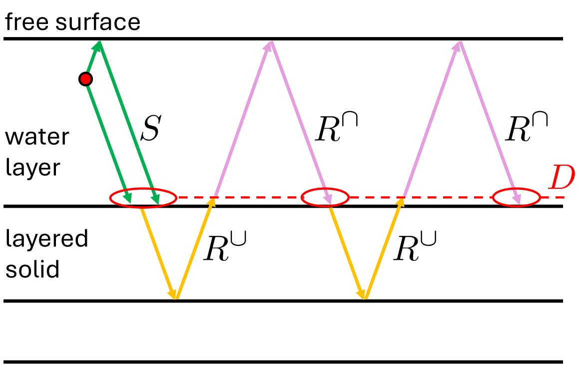

Figure 1. Wavefields in horizontally layered OBS configuration (appearing in equations 1–3). S is the source wavefield (including the free-surface ghost) just above the ocean bottom, and $R^\cap$ is the reflection response of the free surface, seen from just above the ocean bottom. S and $R^\cap$ are defined in the water layer, including the free surface, but with the medium below this layer replaced by a homogeneous half-space (we call this state A). D (indicated by the red ellipses) is the total downgoing field with free-surface multiples, just above the ocean bottom. It is defined in the actual medium, with the free surface (we call this state B). $R^\cup$ is the reflection response of the layered solid medium without free-surface multiples, seen from just above the ocean bottom. It is defined in the actual medium, but with the free surface replaced by a transparent surface (we call this state C).

REPRESENTATION FOR RECEIVER-SIDE DOWN-DOWN DECONVOLUTION

The 1D deconvolution approach breaks down when the medium (above and/or below the ocean bottom) is laterally varying. For this situation, we need a multidimensional version of equation 2, as a basis for multidimensional down-down deconvolution. Similar to multidimensional up-down deconvolution, we derive the new multidimensional representation for down-down deconvolution from reciprocity theorems. In general, reciprocity theorems formulate relations between wavefields in two different states. Fokkema and van den Berg (1993) propose to use such relations for designing seismic processing schemes. For example, if one state is the seismic wavefield with free-surface multiples in the actual earth and the other state is the wavefield in a hypothetical earth without free surface, then exploiting the relation between these wavefields leads to an algorithm for multidimensional surface-related multiple elimination (Van Borselen et al., 1996). In the same realm, we use relations between wavefields in different states to derive a representation for multidimensional down-down deconvolution. However, a complication for deriving a multidimensional version of equation 2 is that the wavefields in this equation are not defined in two, but in three different states (see Figure 1): S and $R^\cap$ are defined in the water layer with the free surface and a homogeneous half-space below this layer (we call this state A), D is defined in the actual medium with the free surface (state B), and $R^\cup$ is defined in the actual medium without the free surface (state C). To deal with these three states, we rewrite equation 2 as follows:

$$D - S = R^\cap U, \quad \text{with} \quad U = R^\cup D, \tag{3}$$

where U is the total upgoing wavefield just above the ocean bottom in the actual medium with the free surface (state B). The first of these equations contains wavefields in states A and B and the second in states B and C. Using reciprocity theory, we separately derive the multidimensional versions of these two equations, which in the end we combine into a multidimensional version of equation 2.

Consider a spatial domain $\mathbb{D}_I$, enclosed by boundaries $\partial\mathbb{D}_0$ (the free surface) and $\partial\mathbb{D}_R$ (just above the ocean bottom), with outward-pointing normal vectors $\mathbf{n} = (n_1, n_2, n_3)$; see states A and B in Figure 2. Boundary $\partial\mathbb{D}_0$ is not necessarily horizontal (to account for a possibly rough sea surface). Note that $\mathbb{D}_I$ corresponds to the water column. In the space-frequency $(\mathbf{x}, \omega)$ domain, the reciprocity theorem for the acoustic wavefields in states A and B reads (Fokkema and van den Berg, 1993)

$$\oint_{\partial\mathbb{D}} \left(p_A v_{k,B} - v_{k,A} p_B \right) n_k \mathrm{d}^2\mathbf{x} = \int_{\mathbb{D}_I} \left(p_A q_B - q_A p_B \right) \mathrm{d}^3\mathbf{x}, \tag{4}$$

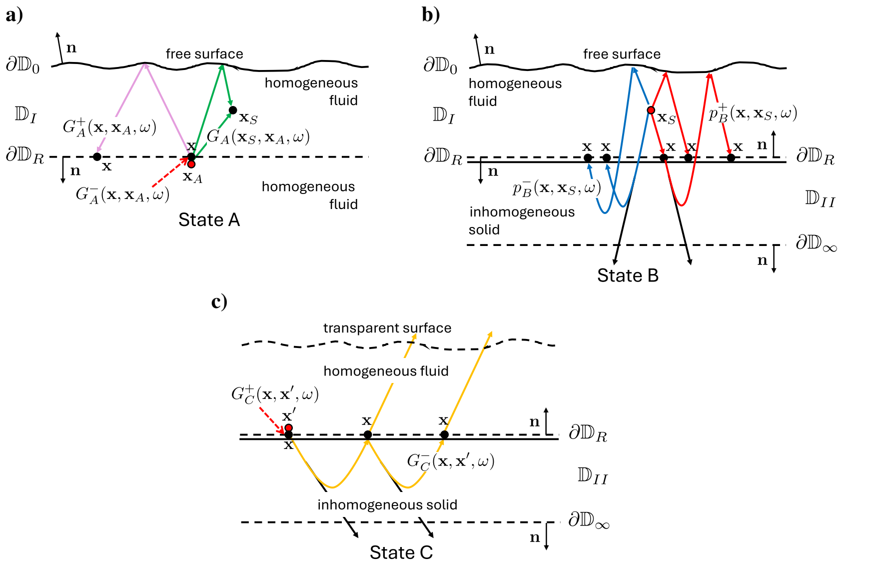

Figure 2. Green's functions, used for the derivation of the receiver-side multidimensional down-down deconvolution representation (equation 9), in an arbitrarily inhomogeneous medium. In state A (the water layer with the free surface and a homogeneous half-space below this layer), Green's function $G_A(\mathbf{x}_S, \mathbf{x}_A, \omega) = G_A(\mathbf{x}_A, \mathbf{x}_S, \omega)$ replaces S and $G_A^+(\mathbf{x}, \mathbf{x}_A, \omega)$ replaces $R^\cap$ in Figure 1. In state B (the actual medium with the free surface), the downgoing wavefield $p_B^+(\mathbf{x}, \mathbf{x}_S, \omega)$ replaces D in Figure 1 (and $p_B^-(\mathbf{x}, \mathbf{x}_S, \omega)$ replaces U in equation 3). In state C (the actual medium without the free surface), Green's function $G_C^-(\mathbf{x}, \mathbf{x}', \omega)$ replaces $R^\cup$ in Figure 1.

where $p(\mathbf{x}, \omega)$ is the acoustic pressure, $v_k(\mathbf{x}, \omega)$ for $k = 1, 2, 3$ the particle velocity, $q(\mathbf{x}, \omega)$ the volume injection-rate density, and $\partial\mathbb{D} = \partial\mathbb{D}_0 \cup \partial\mathbb{D}_R$ (the contribution of the integral over a cylindrical side boundary with infinite radius vanishes). Einstein's summation convention applies to the repeated subscript k. Because the pressure vanishes at the free surface $\partial\mathbb{D}_0$ in both states, the boundary integral can be restricted to $\partial\mathbb{D}_R$, with $n_1 = n_2 = 0$ and $n_3 = +1$ (we assume that the positive x_3-axis is pointing downward). Applying pressure-normalized up-down decomposition at $\partial\mathbb{D}_R$, we obtain (Wapenaar and Berkhout, 1989, Appendix B)

$$-\frac{2}{i\omega\rho}\int_{\partial\mathbb{D}_R}\left((\partial_3 p_A^+)p_B^- + (\partial_3 p_A^-)p_B^+\right)\mathrm{d}^2\mathbf{x} = \int_{\mathbb{D}_I}(p_A q_B - q_A p_B)\mathrm{d}^3\mathbf{x}, \tag{5}$$

where superscripts $+$ and $-$ denote downward and upward propagation, respectively, ρ is the mass density of the water column, i is the imaginary unit, and ∂_3 stands for differentiation in the x_3-direction. Pressure-normalized decomposition implies $p_A^+ + p_A^- = p_A$ and $p_B^+ + p_B^- = p_B$. Note that the derivation of equation 5 from equation 4 relies on the assumption that $\partial\mathbb{D}_R$ is horizontal. The derivation can be extended for flux-normalized decomposed fields at a curved boundary (Frijlink and Wapenaar, 2010), but this is beyond the scope of this paper.

With reference to Figure 2, for state B, we choose the actual medium, and the wavefield in this state is the response to a source $q_B(\mathbf{x}, \omega) = \delta(\mathbf{x} - \mathbf{x}_S)s(\omega)$, with $\mathbf{x}_S$ in $\mathbb{D}_I$ and where $s(\omega)$ is the source signature. Hence, for $\mathbf{x}$ in $\mathbb{D}_I$, we have $p_B(\mathbf{x}, \mathbf{x}_S, \omega) = G_B(\mathbf{x}, \mathbf{x}_S, \omega)s(\omega)$, where $G_B(\mathbf{x}, \mathbf{x}_S, \omega)$ is Green's function in state B. Here and in the following, the second coordinate vector refers to a source position and the first to a receiver position. For $\mathbf{x}$ at $\partial\mathbb{D}_R$, we express $p_B^\pm$ in terms of a pressure-normalized decomposed Green's function, i.e., $p_B^\pm(\mathbf{x}, \mathbf{x}_S, \omega) = G_B^\pm(\mathbf{x}, \mathbf{x}_S, \omega)s(\omega)$, where superscripts $+$ and $-$ denote the downgoing and upgoing components of the wavefield at the receiver position $\mathbf{x}$. For state A, we replace the half-space below $\partial\mathbb{D}_R$ by a homogeneous fluid with the same properties as the fluid above $\partial\mathbb{D}_R$, such that the entire medium below the free surface is homogeneous. We choose a unit source $q_A(\mathbf{x}, \omega) = \delta(\mathbf{x} - \mathbf{x}_A)$, with $\mathbf{x}_A$ just below $\partial\mathbb{D}_R$, i.e., outside $\mathbb{D}_I$. Then, for $\mathbf{x}$ in $\mathbb{D}_I$, we have $p_A(\mathbf{x}, \mathbf{x}_A, \omega) = G_A(\mathbf{x}, \mathbf{x}_A, \omega)$, and for $\mathbf{x}$ at $\partial\mathbb{D}_R$, we consider the decomposed field $p_A^\pm(\mathbf{x}, \mathbf{x}_A, \omega) = G_A^\pm(\mathbf{x}, \mathbf{x}_A, \omega)$. The vertical derivative of the upgoing field for $\mathbf{x}$ at $\partial\mathbb{D}_R$ is nonzero only vertically above $\mathbf{x}_A$, according to $\partial_3 p_A^-(\mathbf{x}, \mathbf{x}_A, \omega) = \partial_3 G_A^-(\mathbf{x}, \mathbf{x}_A, \omega) = -\frac{1}{2}i\omega\rho\delta(\mathbf{x}_\mathrm{H} - \mathbf{x}_{\mathrm{H},A})$ (Wapenaar et al., 2017; Appendix A), where $\mathbf{x}_\mathrm{H}$ and $\mathbf{x}_{\mathrm{H},A}$ denote the horizontal coordinates of $\mathbf{x}$ and $\mathbf{x}_A$, respectively. The downgoing field for $\mathbf{x}$ at $\partial\mathbb{D}_R$ is the "reflection response from below" of the fluid layer above $\partial\mathbb{D}_R$ (bounded by the free surface), according to $\partial_3 p_A^+(\mathbf{x}, \mathbf{x}_A, \omega) = \partial_3 G_A^+(\mathbf{x}, \mathbf{x}_A, \omega) = \frac{1}{2}i\omega\rho R^\cap(\mathbf{x}_A, \mathbf{x}, \omega)$ (note that due to the operator ∂_3 acting on $\mathbf{x}$ and the interchange of $\mathbf{x}$ and $\mathbf{x}_A$, the source at $\mathbf{x}$ in $R^\cap(\mathbf{x}_A, \mathbf{x}, \omega)$ is a dipole source). Substituting these choices into equation 5, using $G_A(\mathbf{x}_S, \mathbf{x}_A, \omega) = G_A(\mathbf{x}_A, \mathbf{x}_S, \omega) = G_A^+(\mathbf{x}_A, \mathbf{x}_S, \omega)$, yields

$$p_B^+(\mathbf{x}_A, \mathbf{x}_S, \omega) - G_A^+(\mathbf{x}_A, \mathbf{x}_S, \omega)\, s(\omega) = \int_{\partial\mathbb{D}_R} R^\cap(\mathbf{x}_A, \mathbf{x}, \omega)\, p_B^-(\mathbf{x}, \mathbf{x}_S, \omega)\, d^2\mathbf{x}. \tag{6}$$

This new representation is, term by term, the multidimensional extension of the first expression in equation 3.

Next, we consider domain $\mathbb{D}_{II}$, enclosed by horizontal boundaries $\partial\mathbb{D}_R$ (just above the ocean bottom) and $\partial\mathbb{D}_\infty$ (below all inhomogeneities in the solid); see states B and C in Figure 2. Hence, $\mathbb{D}_{II}$ consists of a thin fluid domain $\mathbb{D}_f$ (between $\partial\mathbb{D}_R$ and the ocean bottom) and a solid domain $\mathbb{D}_s$ (between the ocean bottom and $\partial\mathbb{D}_\infty$), i.e., $\mathbb{D}_{II} = \mathbb{D}_f \cup \mathbb{D}_s$. This time we start with the reciprocity theorem for a fluid–solid configuration of equation A-1 (with subscripts A replaced by C). Because all elastic wavefields at $\partial\mathbb{D}_\infty$ (which corresponds to $\partial\mathbb{D}_s$ in equation A-1) are outgoing, the boundary integral over $\partial\mathbb{D}_\infty$ vanishes (Pao and Varatharajulu, 1976). If we further assume that $\mathbb{D}_{II}$ is source free in both states, we are left with the boundary integral over $\partial\mathbb{D}_R$ (which corresponds to $\partial\mathbb{D}_f$ in equation A-1) being equal to zero. After up-down decomposition (similar to in equation 5), we thus obtain

$$\frac{2}{i\omega\rho}\int_{\partial\mathbb{D}_R}\Big((\partial_3 p_C^+)p_B^- + (\partial_3 p_C^-)p_B^+\Big)\mathrm{d}^2\mathbf{x} = 0. \tag{7}$$

With reference to Figure 2, for state C, we choose the actual medium, with the free surface replaced by a transparent surface. The wavefield in this state is the response to a unit source $q_C(\mathbf{x},\omega) = \delta(\mathbf{x}-\mathbf{x}')$, with $\mathbf{x}'$ just above $\partial\mathbb{D}_R$, i.e., outside $\mathbb{D}_{II}$. For $\mathbf{x}$ at $\partial\mathbb{D}_R$, we express $p_C^\pm$ as a decomposed Green's function, according to $p_C^\pm(\mathbf{x},\mathbf{x}',\omega) = G_C^\pm(\mathbf{x},\mathbf{x}',\omega)$. The vertical derivative of the downgoing field for $\mathbf{x}$ at $\partial\mathbb{D}_R$ is nonzero only vertically below $\mathbf{x}'$, according to $\partial_3 p_C^+(\mathbf{x},\mathbf{x}',\omega) = \partial_3 G_C^+(\mathbf{x},\mathbf{x}',\omega) = \frac{1}{2}i\omega\rho\delta(\mathbf{x}_\mathrm{H}-\mathbf{x}'_\mathrm{H})$, where $\mathbf{x}'_\mathrm{H}$ denotes the horizontal coordinates of $\mathbf{x}'$. The upgoing field for $\mathbf{x}$ at $\partial\mathbb{D}_R$ is the reflection response of the fluid–solid configuration below $\partial\mathbb{D}_R$, according to $\partial_3 p_C^-(\mathbf{x},\mathbf{x}',\omega) = \partial_3 G_C^-(\mathbf{x},\mathbf{x}',\omega) = -\frac{1}{2}i\omega\rho R^\cup(\mathbf{x}',\mathbf{x},\omega)$. For state B, we make the same choices as before, noting that $\mathbf{x}_S$ is outside $\mathbb{D}_{II}$. Substituting these choices into equation 7 yields

$$p_B^-(\mathbf{x}',\mathbf{x}_S,\omega) = \int_{\partial\mathbb{D}_R} R^\cup(\mathbf{x}',\mathbf{x},\omega)p_B^+(\mathbf{x},\mathbf{x}_S,\omega)\mathrm{d}^2\mathbf{x}. \tag{8}$$

This is the multidimensional extension of the second expression in equation 3, and it coincides with equation 7 in Amundsen et al. (2001) (or equation 17 in Wapenaar et al. (2000)). Substituting equation 8 into equation 6 (with $\mathbf{x}$ replaced by $\mathbf{x}'$) yields

$$\begin{aligned} &p_B^+(\mathbf{x}_A,\mathbf{x}_S,\omega) - G_A^+(\mathbf{x}_A,\mathbf{x}_S,\omega)s(\omega) = \\ &\int_{\partial\mathbb{D}_R}\int_{\partial\mathbb{D}_R} R^\cap(\mathbf{x}_A,\mathbf{x}',\omega)R^\cup(\mathbf{x}',\mathbf{x},\omega)p_B^+(\mathbf{x},\mathbf{x}_S,\omega)\mathrm{d}^2\mathbf{x}\mathrm{d}^2\mathbf{x}'. \end{aligned} \tag{9}$$

This is, term by term, the multidimensional extension of equation 2, where $p_B^+(\mathbf{x},\mathbf{x}_S,\omega)$ stands for the measured total downgoing wavefield and $G_A^+(\mathbf{x}_A,\mathbf{x}_S,\omega)s(\omega)$ for the modeled downgoing source wavefield (including the free-surface ghost) at $\partial\mathbb{D}_R$, just above the ocean bottom. This new representation forms a basis for receiver-side multidimensional down-down deconvolution, aiming to retrieve the reflection response $R^\cup$ at $\partial\mathbb{D}_R$ of the inhomogeneous solid, without free-surface multiples. This generalizes existing 1D down-down deconvolution approaches based on equation 2. In practice, all quantities in equation 9 are discretized in space, and the integrals become matrix products. Hence, in practice, multidimensional down-down deconvolution involves matrix inversion per frequency component. Pros and cons relative to other multidimensional deconvolution methods are discussed in the discussion section.

REPRESENTATION FOR SOURCE-SIDE DOWN-DOWN DECONVOLUTION

The representation of equation 9 contains integrals over receivers at $\partial\mathbb{D}_R$. Because receivers are often sparsely sampled in OBS acquisition, Boiero et al. (2023) and Wang and Ravasi (2024) derive representations for down-down deconvolution, containing an integral over the sources. Here, we derive such a representation, using the formalism of the previous section, to facilitate the comparison between the two approaches.

Consider a domain $\mathbb{D}_f \cup \mathbb{D}_s$ (where subscripts f and s stand for fluid and solid, respectively), enclosed by horizontal boundaries $\partial\mathbb{D}_S$ (just below the sources in the fluid) and $\partial\mathbb{D}_\infty$ (below all inhomogeneities in the solid) (see Figure 3). Because in the following derivations we do not encounter integrals along the receivers at the ocean bottom, there is no need to assume that the ocean bottom (the boundary between $\mathbb{D}_f$ and $\mathbb{D}_s$) is horizontal. We use again the reciprocity theorem of equation A-1 for the fluid–solid configuration. As before, the boundary integral over $\partial\mathbb{D}_\infty$ (which corresponds to $\partial\mathbb{D}_s$ in equation A-1) vanishes. Assuming the solid domain $\mathbb{D}_s$ is source free, we are left with a boundary integral over $\partial\mathbb{D}_S$ (which corresponds to $\partial\mathbb{D}_f$ in equation A-1) and a domain integral over $\mathbb{D}_f$. Applying pressure-normalized up-down decomposition, this time not only to the wavefields but also to the sources (Wapenaar, 2020), we thus have

$$\begin{aligned} &\frac{2}{i\omega\rho}\int_{\partial\mathbb{D}_S}\Big((\partial_3 p_A^+)p_B^- + (\partial_3 p_A^-)p_B^+\Big)\mathrm{d}^2\mathbf{x} = \\ &\int_{\mathbb{D}_f}\Big(p_A^+q_B^- + p_A^-q_B^+ - q_A^+p_B^- - q_A^-p_B^+\Big)\mathrm{d}^3\mathbf{x}. \end{aligned} \tag{10}$$

In state A (the actual medium, but with a transparent surface), we choose a unit source for downgoing waves $q_A^+(\mathbf{x},\omega) = \delta(\mathbf{x}-\mathbf{x}_S)$ (and $q_A^-(\mathbf{x},\omega) = 0$), with $\mathbf{x}_S$ just above $\partial\mathbb{D}_S$, hence, outside $\mathbb{D}_f$. Hence, in the fluid, we have $p_A^\pm(\mathbf{x},\mathbf{x}_S,\omega) = G_A^{\pm,+}(\mathbf{x},\mathbf{x}_S,\omega)$, where the second superscript $+$ denotes that the source at $\mathbf{x}_S$ radiates downward. For $\mathbf{x}$ at $\partial\mathbb{D}_S$, we have $\partial_3 p_A^+(\mathbf{x},\mathbf{x}_S,\omega) = \partial_3 G_A^{+,+}(\mathbf{x},\mathbf{x}_S,\omega) = \frac{1}{2}i\omega\rho\delta(\mathbf{x}_\mathrm{H}-\mathbf{x}_{\mathrm{H},S})$ (where $\mathbf{x}_{\mathrm{H},S}$ denotes the horizontal coordinates of $\mathbf{x}_S$) and $\partial_3 p_A^-(\mathbf{x},\mathbf{x}_S,\omega) = \partial_3 G_A^{-,+}(\mathbf{x},\mathbf{x}_S,\omega) = -\frac{1}{2}i\omega\rho R^\cup(\mathbf{x}_S,\mathbf{x},\omega)$ (where $R^\cup(\mathbf{x}_S,\mathbf{x},\omega)$ is the reflection response of the fluid–solid configuration below $\partial\mathbb{D}_S$). In state B (the actual medium with the free surface), we choose a source for upgoing waves $q_B^-(\mathbf{x},\omega) = \delta(\mathbf{x}-\mathbf{x}_A)s(\omega)$ (and $q_B^+(\mathbf{x},\omega) = 0$), with $\mathbf{x}_A$ just above the ocean bottom, hence, inside $\mathbb{D}_f$. Hence, in the fluid, we have $p_B^{\pm,-}(\mathbf{x},\mathbf{x}_A,\omega) = G_B^{\pm,-}(\mathbf{x},\mathbf{x}_A,\omega)s(\omega)$, where the second superscript $-$ denotes that the source at $\mathbf{x}_A$ radiates upward. Substituting these choices into equation 10, using the pressure-normalized source–receiver reciprocity relations $G_B^{+,-}(\mathbf{x},\mathbf{x}_A,\omega) = G_B^{+,-}(\mathbf{x}_A,\mathbf{x},\omega)$ and $G_B^{-,-}(\mathbf{x},\mathbf{x}_A,\omega) = G_B^{+,+}(\mathbf{x}_A,\mathbf{x},\omega)$ (Wapenaar, 2020), yields

$$p_B^{+,+}(\mathbf{x}_A, \mathbf{x}_S, \omega) - G_A^{+,+}(\mathbf{x}_A, \mathbf{x}_S, \omega)s(\omega) = \int_{\partial\mathbb{D}_S} R^{\cup}(\mathbf{x}_S, \mathbf{x}, \omega)p_B^{+,-}(\mathbf{x}_A, \mathbf{x}, \omega)\mathrm{d}^2\mathbf{x}, \tag{11}$$

where $p_B^{+,\pm}(\mathbf{x}_A, \mathbf{x}, \omega) = G_B^{+,\pm}(\mathbf{x}_A, \mathbf{x}, \omega)s(\omega)$ for all $\mathbf{x}$ at $\partial\mathbb{D}_S$. This representation forms the basis for source-side multidimensional down-down deconvolution, aiming to retrieve the reflection response $R^{\cup}$ at $\partial\mathbb{D}_S$ of the fluid–solid configuration, without free-surface multiples. The main difference with equation 9 is that here the integral is taken over the sources at $\mathbf{x}$ at $\partial\mathbb{D}_S$ instead of over the receivers at $\partial\mathbb{D}_R$ and that these sources are decomposed into downward- and upward-radiating components. Furthermore, note that the downgoing source wavefield $G_A^{+,+}(\mathbf{x}_A, \mathbf{x}_S, \omega)s(\omega)$ does not include the free-surface ghost, unlike the downgoing source wavefield $G_A^{+}(\mathbf{x}_A, \mathbf{x}_S, \omega)s(\omega)$ in equation 9. Apart from notational differences, the representation of equation 11 corresponds to those of Boiero et al. (2023) and Wang and Ravasi (2024).

DISCUSSION

We discuss here the pros (+) and cons (−) of applying the representations derived in this paper to ocean-bottom data, typically acquired for seismic exploration projects.

Equation 8, i.e., the representation underlying the traditional multidimensional up-down deconvolution method, provides the perfect setup to obtain the receiver-to-receiver response $R^{\cup}(\mathbf{x}', \mathbf{x}, \omega)$ in a fully data-driven manner. Given that the integral to be inverted is along the receiver array:

+ It does not require any knowledge of the source locations and wavelets; as such, it can theoretically handle any complex source signature (including multiple sources firing together — also known as blended data acquisition).

+ It can handle complexity in the "overburden" (e.g., a rough sea surface), making it ideal for 4D compliant processing.

− It requires a densely sampled receiver array.

The new representation underlying the receiver-side down-down deconvolution scheme (equation 9), being also formulated as a spatial integral over the receiver array, shares most of the pros and cons of equation 8; however, it has some additional pros and cons:

+ It uses only the downgoing part of the wavefield that better samples the shallow subsurface.

− It relies on accurate modeling of the downgoing source wavefield (including the free-surface ghost) and of the reflection response $R^{\cap}(\mathbf{x}_A, \mathbf{x}', \omega)$ of the water layer from below, which in turn requires knowledge of the acoustic properties of the water layer and accurate measurements of the source and receiver positions; in addition, rough sea conditions can further affect the accurate modeling of $G_A^{+}(\mathbf{x}_A, \mathbf{x}_S, \omega)s(\omega)$ and $R^{\cap}(\mathbf{x}_A, \mathbf{x}', \omega)$, which needs to be repeated when the conditions change during a survey.

On the other hand, the representation underlying the source-side down-down deconvolution scheme (equation 11) involves an integration over the source array. It has the following pros and cons:

+ For economic reasons, the source array is more densely sampled than the receiver array; hence, discretization of the source integral in equation 11 is more accurate than that of the receiver integrals in equations 8 and 9.

+ It accounts for an arbitrarily shaped ocean bottom.

− Because the integration is carried out over sources, it cannot handle blended data, all source signatures need to be the same, and the sea surface should not change during a survey.

− Similar to equation 9, because it relies on a model-based downgoing source wavefield $G_A^{+,+}(\mathbf{x}_A, \mathbf{x}_S, \omega)s(\omega)$, its inversion is not fully data driven and therefore less 4D friendly than equation 8.

− It requires that the downgoing wavefield $p_B^{+}(\mathbf{x}_A, \mathbf{x}_S, \omega)$ is decomposed into a wavefield $p_B^{+,+}(\mathbf{x}_A, \mathbf{x}_S, \omega)$ due to a source radiating downward and a wavefield $p_B^{+,-}(\mathbf{x}_A, \mathbf{x}_S, \omega)$ due to a source radiating upward; in other words, the seismic processing step often referred to as "source deghosting" in the seismic exploration community is required.

− In the presence of sparsely sampled receiver arrays (or nodes), it represents an underdetermined system of linear equations whose solution requires regularization (Boiero and Bagaini, 2021; Ravasi and Vasconcelos, 2025).

Finally, it is worth noting that when receiver-side equations 8 and 9 are approximately solved in a 1D fashion, this is conventionally accomplished in the receiver gather domain; however, our derivation shows that both schemes require dense receiver arrays when treated in a multidimensional fashion. As such, although the argument of using

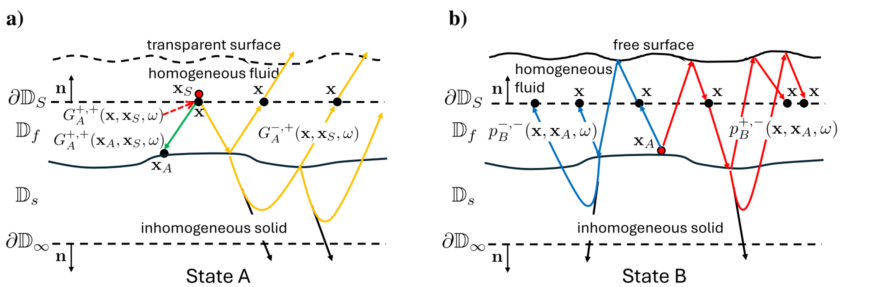

Figure 3. Green's functions, used for the derivation of the source-side multidimensional down-down deconvolution representation (equation 11), in an arbitrarily inhomogeneous medium. In state A (the actual medium without the free surface), Green's function $G_A^{+,+}(\mathbf{x}_A, \mathbf{x}_S, \omega)$ is the downgoing source wavefield (without the free-surface ghost) at $\mathbf{x}_A$ just above the ocean bottom, and $G_A^{-,+}(\mathbf{x}, \mathbf{x}_S, \omega)$, with $\mathbf{x}$ at $\partial\mathbb{D}_S$, represents the reflection response of the fluid-solid configuration, without free-surface multiples. In state B (the actual medium with the free surface), $p_B^{\pm,-}(\mathbf{x}, \mathbf{x}_A, \omega)$ represents the downgoing (+) and upgoing (−) wavefield at $\mathbf{x}$ at $\partial\mathbb{D}_S$, in response to an upward-radiating source at $\mathbf{x}_A$. After applying reciprocity, $p_B^{+,\mp}(\mathbf{x}_A, \mathbf{x}, \omega)$ represents the downgoing wavefield at $\mathbf{x}_A$ just above the ocean bottom, in response to upward (−) and downward (+) radiating sources at $\mathbf{x}$ at $\partial\mathbb{D}_S$.

equation 9 over equation 8 to leverage the superior illumination of the downgoing wavefield over the upgoing wavefield in the presence of sparse receiver geometries is meaningful in 1D, it falls short in a multidimensional setting due to the need for a dense receiver array in the spatial integral.

CONCLUSION

We have derived different representation theorems as bases for suppressing free-surface effects and redatuming seabed seismic data by deconvolving different components of the recorded wavefield. In theory (i.e., under ideal acquisition conditions), the traditional receiver-side up-down multidimensional deconvolution scheme is the most appealing in that it is fully data driven. The recently proposed source-side down-down deconvolution scheme represents an important alternative in the presence of sparse receiver geometries (when a preprocessing step of receiver interpolation is not an option), although it requires more careful preprocessing and is no longer fully data driven. On the other hand, our derivation of the representation for multidimensional receiver-side down-down deconvolution shows that, because of its reliance on a spatial integral over the receiver array, receiver-side down-down deconvolution shares the same challenges as the traditional up-down deconvolution method when applied to data acquired with sparse receiver geometries for seismic exploration projects.

DATA AND MATERIALS AVAILABILITY

No data have been used for this paper.

APPENDIX A: RECIPROCITY THEOREM FOR A FLUID–SOLID CONFIGURATION

Consider the fluid–solid configuration of Figure A-1. It consists of a domain $\mathbb{D}_f$, containing an inhomogeneous fluid, and a domain $\mathbb{D}_s$, containing an inhomogeneous solid. These domains are coupled at a fluid–solid interface. Acoustic and elastodynamic reciprocity theorems hold for domains $\mathbb{D}_f$ and $\mathbb{D}_s$, respectively. Summing the left- and right-hand sides of these theorems, taking into account that the boundary integrals along the interface cancel each other, de Hoop (1990) and Pandey et al. (2025) obtain the following reciprocity theorem for the fluid–solid configuration:

$$\begin{aligned}&\int_{\partial\mathbb{D}_f}(p_A v_{k,B} - v_{k,A}p_B)n_k\,d^2\mathbf{x}\\&\quad+\int_{\partial\mathbb{D}_s}(-\tau_{kl,A}v_{k,B} + v_{k,A}\tau_{kl,B})n_l\,d^2\mathbf{x}\\&=\int_{\mathbb{D}_f}(p_A q_B - q_A p_B - v_{k,A}f_{k,B} + f_{k,A}v_{k,B})d^3\mathbf{x}\\&\quad+\int_{\mathbb{D}_s}(-\tau_{kl,A}h_{kl,B} + h_{kl,A}\tau_{kl,B} - v_{k,A}f_{k,B} + f_{k,A}v_{k,B})d^3\mathbf{x},\end{aligned} \tag{A-1}$$

where $\partial\mathbb{D}_f$ and $\partial\mathbb{D}_s$ (with outward-pointing normal vector $\mathbf{n} = (n_1, n_2, n_3)$) are the boundaries of $\mathbb{D}_f$ and $\mathbb{D}_s$, respectively, both excluding the interface (hence, $\partial\mathbb{D}_f \cup \partial\mathbb{D}_s$ encloses the total domain $\mathbb{D}_f \cup \mathbb{D}_s$; see Figure A-1). Subscripts A and B refer again to two different states, p, v_k, and q are defined the same as in equation 4, τ_{kl} is the stress tensor, f_k is the external force density, and h_{kl} is the deformation-rate density tensor.

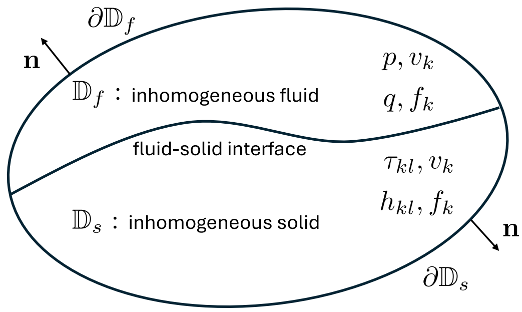

Figure A-1. Fluid–solid configuration, underlying the reciprocity theorem of equation A-1. In Figure 2, $\partial\mathbb{D}_f = \partial\mathbb{D}_R$ is chosen just above the ocean bottom, and in Figure 3, $\partial\mathbb{D}_f = \partial\mathbb{D}_S$ is chosen just below the sources in the water layer. In both figures, $\partial\mathbb{D}_s = \partial\mathbb{D}_\infty$ is chosen below all inhomogeneities in the solid.

REFERENCES

Amundsen, L., 1999, Elimination of free surface-related multiples without need of the source wavelet: 69th Annual International Meeting, SEG, Expanded Abstracts, 1064–1067. doi: 10.1190/1.1820682.

Amundsen, L., L. T. Ikelle, and L. E. Berg, 2001, Multidimensional signature deconvolution and free-surface multiple elimination of marine multicomponent ocean-bottom seismic data: Geophysics, **66**, 1594–1604, doi: 10.1190/1.1486770.

Boiero, D., and C. Bagaini, 2021, Up and down deconvolution in complex geological scenarios: Geophysics, **86**, no. 5, WC55–WC65, doi: 10.1190/geo2020-0926.1.

Boiero, D., S. Mahat, C. Bagaini, and M. Ortin, 2023, True-amplitude multiple prediction in sparse ocean-bottom acquisitions using a multidimensional deconvolution approach: 84th Annual International Meeting, EAGE, Extended Abstracts, 1–5. doi: 10.3997/2214-4609.202310695.

Caprioli, P., and P. Kristiansen, 2021, Data-driven prediction of downgoing free-surface multiples for ocean-bottom node data: 82nd Annual International Meeting, EAGE, Extended Abstracts, 1–5. doi: 10.3997/2214-4609.202113235.

de Hoop, A. T., 1990, Reciprocity theorems for acoustic wave fields in fluid/solid configurations: The Journal of the Acoustical Society of America, **87**, 1932–1937, doi: 10.1121/1.399319.

Fokkema, J. T., and P. M. van den Berg, 1993, Seismic applications of acoustic reciprocity: Elsevier, Amsterdam.

Frijlink, M., and K. Wapenaar, 2010, Reciprocity theorems for one-way wave fields in curvilinear coordinate systems: SIAM Journal on Imaging Sciences, **3**, no. 3, 390–415, doi: 10.1137/080739185.

Hampson, G., and G. Szumski, 2020, Down/down deconvolution: EAGE Seabed Seismic Today: from Acquisition to Application, 1–5. doi: 10.3997/2214-4609.2020611022.

Lokshtanov, D., E. Sadikhov, and M. N. Ab Ghani, 2024, Practical aspects of fast and efficient UDD and DDD for OBS data: 85th Annual International Meeting, EAGE, Extended Abstracts, 1–5. doi: 10.3997/2214-4609.202410975.

Pandey, A., S. de Ridder, J. Shragge, and A. J. Girard, 2025, Ocean-bottom seismic interferometry in coupled acoustic–elastic media: Geophysical Journal International, **242**, ggaf271, doi: 10.1093/gji/ggaf271.

Pao, Y. H., and V. Varatharajulu, 1976, Huygens' principle, radiation conditions, and integral formulas for the scattering of elastic waves: The Journal of the Acoustical Society of America, **59**, 1361–1371, doi: 10.1121/1.381022.

Ravasi, M., and I. Vasconcelos, 2025, Regularising time-domain multi-dimensional deconvolution with offset-directional derivatives: 86th Annual International Meeting, EAGE, Extended Abstracts, 1–5. doi: 10.3997/2214-4609.202510416.

Sonneland, L., and L. E. Berg, 1987, Comparison of two approaches to water layer multiple attenuation by wave field extrapolation: 57th

Annual International Meeting, SEG, Expanded Abstracts, 276–277. doi: 10.1190/1.1892114.
Van Borselen, R. G., J. T. Fokkema, and P. M. van den Berg, 1996, Removal of surface-related wave phenomena-The marine case: Geophysics, **61**, 202–210, doi: 10.1190/1.1443940.
Wang, N., and M. Ravasi, 2024, Upside-down Rayleigh-Marchenko: A practical redatuming scheme for seabed seismic acquisitions: Geophysics, **89**, no. 6, V619–V634, doi: 10.1190/geo2023-0743.1.
Wapenaar, K., 2020, Reciprocity and representation theorems for flux- and field-normalised decomposed wave fields: Advances in Mathematical Physics, **2020**, 9540135, doi: 10.1155/2020/9540135.
Wapenaar, C. P. A., and A. J. Berkhout, 1989, Elastic wave field extrapolation: Elsevier, Amsterdam.
Wapenaar, K., J. Fokkema, M. Dillen, and P. Scherpenhuijsen, 2000, One-way acoustic reciprocity and its applications in multiple elimination and time-lapse seismics: 70th Annual International Meeting, SEG, Expanded Abstracts, 2377–2380. doi: 10.1190/1.1815939.
Wapenaar, K., J. Thorbecke, J. van der Neut, E. Slob, and R. Snieder, 2017, Review paper: Virtual sources and their responses, Part II: Data-driven single-sided focusing: Geophysical Prospecting, **65**, 1430–1451, doi: 10.1111/1365-2478.12495.

Biographies and photographs of the authors are not available.